A-1.3.2 Studies on Chemical Reactions and Heterogeneous Processes related to Stratospheric Ozone Depletion

Contact Person Takashi Imamura
Senior Researcher, Atmospheric Environment Division
National Institute for Environmental Studies
Environment Agency
Onogawa, Tsukuba, Ibaraki 305, Japan
Phone +81-298-50-2406, Fax +81-298-51-4732
E-mail imamura@nies.go.jp

Total Budget for FY1993 - FY1995 34,646,000 Yen (FY1995; 12,161,000 Yen)

Abstract

To clarify the effects of the stratospheric sulfate aerosols on the ozone layer, radical reactions related to formation of sulfuric acid, radical-radical reactions including ClO and BrO, uptake coefficients of OH radical to aqueous solutions are examined using photoionization mass spectrometer, photochemical chamber and laser induced fluorescence technique. Simulations of the effects of volcanic aerosols on the ozone layer were also carried out using two types of one dimensional models, an ordinary one dimensional model with heterogeneous reactions and a full interactive one-dimensional model without heterogeneous reactions. By these studies, following major findings were obtained. A radical reaction HS+O → H+SO is important for formation of sulfuric acid. Some specific behavior of OH on the surface, acidity and low temperature seam to be important for uptaking process of OH to aqueous solutions. In the case of the volcanic eruptions like Mt. Pinatubo, ozone reduction due to heterogeneous reactions and due to radiative-chemical coupled processes are 8% (at 20 km) and 2-3% (at 30 km), respectively.

Key Words Heterogeneous Reactions, Radical Reactions, sulfuric Aerosols, HS Radicals, OH Radicals, uptake coefficients, One dimensional Models

1. Introduction

To understand and predict the change of the ozone layer, the knowledge on the heterogeneous chemistry and related radical reactions related to the Polar Stratospheric Clouds (PSCs) and the stratospheric sulfuric acid aerosols are crucial. The processes to be examined include radical radical reactions related to ClO and BrO, related to formation of sulfuric acid and uptake processes of radicals to sulfuric acid aerosols (solutions). In this section we will describe the results of studies mentioned above and the results of simulations on the effects of heavy stratospheric sulfuric acid aerosols on the ozone layer using 1-D models.

2.Experimental Studies of Ozone Depletion by Chlorofluorocarbons, Bromofluorocarbons and CH_3Br using a 6-m^3 Photochemical Chamber

Since the first prediction by Molina and Rowland, it is well known that stratospheric ozone is destroyed by a catalytic cycle involving Cl or Br atoms released from the photolysis of chlorofluorocarbons (CFC's) or bromofluorocarbons (BFC's) by sunlight. Studies concerning the destruction of stratospheric ozone have been carried out involving the determination of the rate constants and reaction mechanisms of the photodecomposition of the CFC's and BFC's as well as the elementary processes of the catalytic reactions, also, computer model calculations based on a variety of scenarios were made.

However, ozone depletion due to such catalytic reactions has never been demonstrated. In the present study, experiments concerning ozone depletion were carried out in a 6-m^3 evacuable photochemical chamber, in which selected CFC's and BFC's were added to about 5

ppm O3 diluted in about 50 Torr air and irradiated by UV light.

1). Measurements of the photodissociation rates of CFC's, BFC's, HCFC's and CH3Br.

First, measurements of the photodissociation rates of the halocarbons used in this study by irradiating Xe arc lamps were determined under the condition of 100 Torr N2. The results for the CFC's and BFC's are shown in Fig.1. The initial concentrations of CF2Cl2, CF3Br, CFCl3, and C2F4Br2 were 3.8, 19.2, 19.4, and 3.0 ppm, respectively. The decreases in the concentrations were measured by IR absorption. Fig.1, gives the values of the relative IR transmittance (It/I0), which are plotted against irradiation time (the scale of the ordinate is logarithmic). Here, I0 stands for the absorption before irradiation and It represents the absorption at the irradiation time (t). From the slopes shown in Fig.1, the photodissociation rates (Jx) of CF2Cl2, CF3Br, CFCl3, and C2F4Br2 were obtained to be (1.2 $\pm$ 0.1) $\times$ 10^{-4}, (4.4 $\pm$ 0.1) $\times$ 10^{-4}, (7.3 $\pm$ 0.4) $\times$ 10^{-4}, and (5.0 $\pm$ 0.1) $\times$ 10^{-3} min^{-1}, respectively. The photodissociation processes of the above compounds are thought to be as follows:

$$CF_2Cl_2 + h\nu \rightarrow CF_2Cl + Cl \quad (1)$$

$$CF_3Br + h\nu \rightarrow CF_3 + Br \quad (2)$$

$$CFCl_3 + h\nu \rightarrow CFCl_2 + Cl \quad (3)$$

$$C_2F_4Br_2 + h\nu \rightarrow C_2F_4Br + Br \quad (4)$$

The photodecomposition rates of CH3CFCl2, CF3CHCl2, CF3CHFCl, and CH3Br were measured in the H2/air system. The photodissociation rates (Jx) of CH3CFCl2, CF3CHCl2, CF3CHFCl, CH3Br, and CFCl3(for reference) are (1.2 $\pm$ 0.1) $\times$ 10^{-3}, (1.1 $\pm$ 0.1) 10^{-3}, (1.9 $\pm$ 0.5) $\times$ 10^{-4}, (6.9 $\pm$ 0.4) $\times$ 10^{-3}, and (2.3 $\pm$ 0.2) $\times$ $10^{-3}min^{-1}$, respectively.

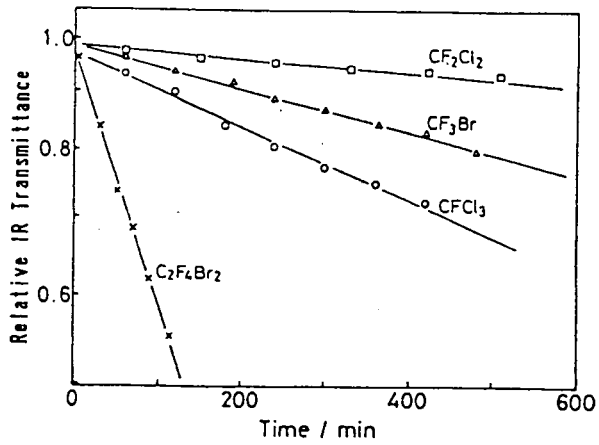

Fig. 1. Relative IR transmittance (I_t/I_0) are plotted against irradiation time (t) (scale of ordinate is logarithmic). Symbols; CF_2Cl_2 (□), CF_3Br (△), $CFCl_3$ (○), and $C_2F_4Br_2$ (×).

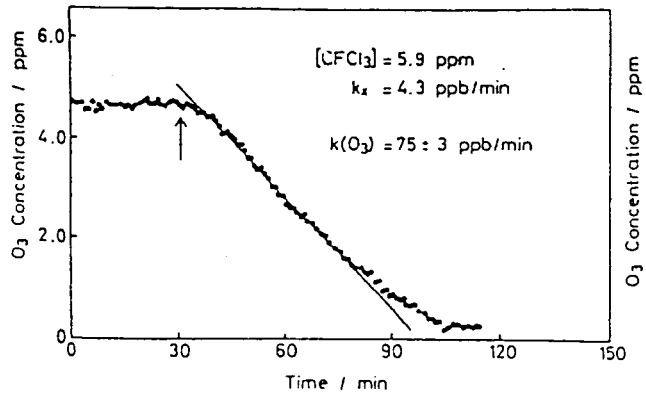

Fig. 2. Decay of the photostationary state concentration of ozone by the addition of 5.9 ppm of $CFCl_3$. $CFCl_3$ was added at the time shown by an arrow. Slope gives the decay rate ($k(O_3)$=75±3 ppb/min).

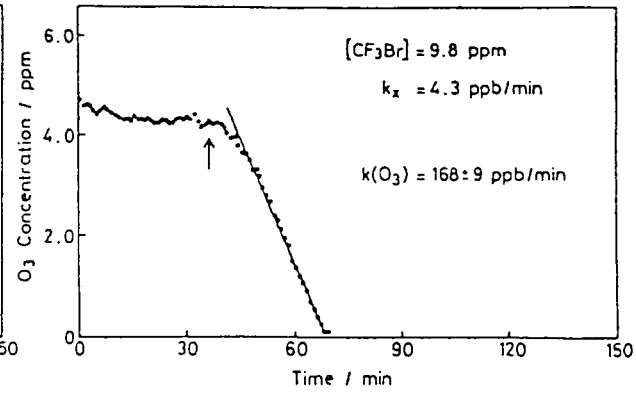

Fig. 3. Decay of the photostationary state concentration of ozone by the addition of 9.8 ppm of CF_3Br. Formation rate of Br, k_x was adjusted to be as same as the case of $CFCl_3$ (Fig. 4). CF_3Br was introduced at the time show by an arrow. Slope gives the decay rate ($k(O_3)$=168±9 ppb/min).

Table 1. Results of the Photodecomposition Rate (J_x) and Ozone Decay Rate ($k(O_3)$)

	$[CFC]_0$	$[O_3]_0$	J_x	k_x	$k(O_3)$	$R(O_3)$	α
	ppm	ppm	min^{-1}	ppb/min	ppb/min		
Run 1							
$CFCl_3$ (CFC-11)	5.86	4.40	$(7.3\pm0.4)\times10^{-4}$	4.3±0.2	75±3	17.4	1
CF_2Cl_2 (CFC-12)	35.69	4.61	$(1.2\pm0.1)\times10^{-4}$	4.3±0.4	72±3	16.7	1.0
CF_3Br (H-1301)	9.78	4.61	$(4.4\pm0.1)\times10^{-4}$	4.3±0.1	168±9	39.1	2.2
$C_2F_4Br_2$ (H-2402)	0.85	4.26	$(5.0\pm0.1)\times10^{-3}$	4.3±0.1	216±19	50.2	2.9
Run 2							
$CFCl_3$ (CFC-11)	3.92	7.67	$(2.3\pm0.2)\times10^{-3}$	9.1±0.8	152±4	16.7	1
CH_3CFCl_2 (HCFC-141b)	7.00	7.96	$(1.2\pm0.1)\times10^{-3}$	8.3±0.7	160±6	19.3	1.2
CF_3CHCl_2 (HCFC-123)	8.89	8.39	$(1.1\pm0.1)\times10^{-3}$	9.8±0.9	94±3	9.6	0.6
CF_3CHFCl (HCFC-124)	49.30	8.55	$(1.9\pm0.5)\times10^{-4}$	9.2±2.4	82±3	9.0	0.5
CH_3Br (Methyl bromide)	1.36	8.45	$(6.9\pm0.4)\times10^{-3}$	9.4±0.5	312±10	33.2	2.0

2). Measurements of the decay rates of ozone by the CFC's, BFC's, HCFC's, and CH3Br.

When a halocarbon was added to the photostationary state concentration (PSSC) of ozone (described in Experimental section) under irradiation, a depletion of ozone, probably caused by the Cl or Br atom catalyzed chain reactions (5) and (6), was observed.

$$X + O3 \rightarrow XO + O2 \qquad (5)$$

$$XO + O \rightarrow X + O2 \qquad (6)$$

where, X is Cl or Br atoms.

The results obtained after adding CFCl3 and CF3Br to the PSSC of O3 are shown in Figs.2 and 3. After a short induction period, ozone was destroyed rapidly in both cases. The concentrations of added CFCl3(5.9 ppm) and CF3Br(9.8 ppm) were adjusted so as to give the same formation rate for Cl and Br by the photodecomposition of CFCl3 and CF3Br(kx=Jx · [halocarbon]= 4.3 ppb · min^{-1}). Where ppb is 10^{-3}ppm. As can be seen in Figs.2 and 3, the effective ozone-depletion rate is faster in CF3Br than in CFCl3. From the slopes of the effective decay of ozone, the decay rates, (k(O3)) were obtained to be 75 ± 3 and 168 ± 9 ppb·min^{-1} for CFCl3 and CF3Br, respectively.

The values of R(O3) given in Table 1 are the ratio of k(O3) to kx,(k(O3)/kx), which indicates the number of ozone molecules decomposed per one Cl or Br atom produced by the photodissociation of the CFC's or BFC's. The number of R(O3) was about 17 for CFCl3 and CF2Cl2, and 40-50 for CF3Br and C2F4Br2. These results show that a Cl atom formed in the chamber could destroy 17 ozone molecules on the average while traveling to the wall of the chamber (on the wall of the chamber Cl atoms might be lost). In the case of the Br atom, 40-50 ozone molecules were destroyed by one Br atom during the traveling time (the photochemical chamber was a cylinder, 1450 mm in diameter, 3500 mm long, and 6065 L in volume, and gases are stirred by two stirring fans). The ozone decomposition efficiency, (R(O3)), were almost equal in CFCl3 and CF2Cl2 under the present experimental conditions. Since the formations of CFClO and CF2O were observed as detectable reaction products by the FTIR spectrometer in systems of CFCl3 and CF2Cl2, respectively, two Cl atoms might have been released from both CFCl3 and CF2Cl2 after photodecomposition by reactions (1) and (3). For example, the following reactions might have occurred:

$CF_2Cl + O_2 + M \rightarrow CF_2ClO_2$ (7)

$2CF_2ClO_2 \rightarrow 2CF_2ClO^{\neq} + O_2$ (8)

$CF_2ClO^{\neq} \rightarrow CF_2O + Cl$ (9)

In any case, it is evident that ozone was destroyed by a catalytic cycle involving Cl or Br atoms.

The large ozone decomposition efficiency of Br compared to that of Cl might be explained by the efficiency to release Cl or Br atoms through radical-radical reactions of ClO and BrO.

$ClO + ClO \rightarrow ClOO + Cl$ (10a)

$\rightarrow OClO + Cl$ (10b)

$\rightarrow Cl_2 + O_2$ (10c)

$BrO + BrO \rightarrow 2Br + O_2$ (11a)

$\rightarrow Br_2 + O_2$ (11b)

The rate constant for reaction (11), $2.7 \times 10^{-12} cm^3 molecule^{-1} s^{-1}$, is much faster than reaction (10), $1.0 \times 10^{-14} cm^3 molecule^{-1} s^{-1}$, and the branching ratios in reactions (10) and (11) are: f (10a):f (10b) : f (10c)=0.34 : 0.17 : 0.49 and f (11a) : f (11b) =0.83 : 0.17. Therefore, the efficiency of reproducing halogen atoms through a radical-radical reaction is 8.6×10^2 times larger in reaction (11) than in reaction (10). The longer chain length in Br atoms (40-50) than that of Cl atoms (6) can be qualitatively understood based on reactions (10) and (11). However, it is not easy to elucidate the meaning of the quantitative difference between both chain lengths. Trial box-model simulations were investigated in order to understand the mechanism of the catalytic chain reactions. In these simulations, the decay phenomena had to be adjusted by the rate of the wall reactions for $O(^3P)$, Cl, Br, ClO, BrO and RO2:

$O(^3P) + wall \rightarrow$ removal of $O(^3P)$ (12)

$Cl + wall \rightarrow$ removal of Cl (13)

$Br + wall \rightarrow$ removal of Br (14)

$ClO + wall \rightarrow$ removal of ClO (15)

$BrO + wall \rightarrow$ removal of BrO (16)

$RO_2 + wall \rightarrow$ removal of RO2 (17)

3). Box model simulation

Figure 4 shows the result of a trial box-model simulation of the O3+CFCl3+h ν system shown in Fig.2. In this figure the concentrations of O3 in units of 10^{12} molecule $\cdot$ cm^{-3} (not ppm) are plotted against the reaction time (time zero is the point shown by the arrow in Fig.2). Calculations were carried out using 42 reactions for 19 chemical species (molecules and radicals). The circles in Fig.4 indicate the experimental results shown in Fig.2. The dotted line shows the result of a simulation without wall-loss processes for all of the chemical species. The solid line indicates the case including wall-loss processes of $O(^3P)$, Cl, ClO, and RO2 (2×10^{-3} sec^{-1} was used as wall-loss rates for all four species). As can be seen in Fig.4, if wall-loss processes are neglected, the decay of O3 obtained is much faster than the experi-

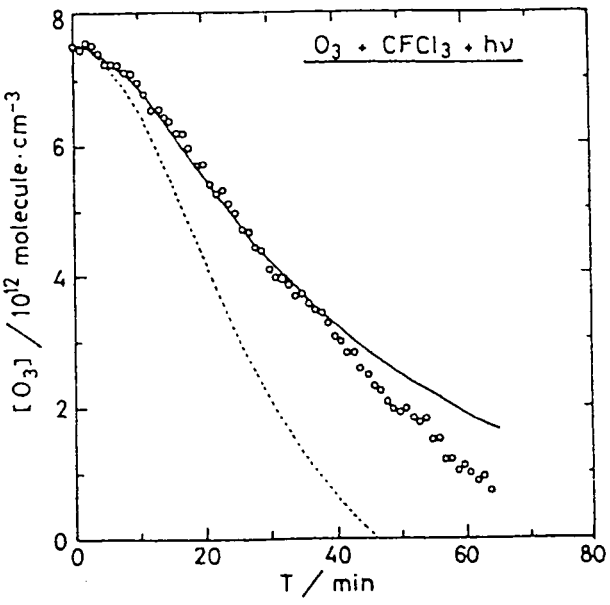

Fig. 4. Results of box model simulation of the $O_3+CFCl_3+h\nu$ system. Circles show experimental results shown in Fig. 4. The dotted line shows the result of simulation without wall loss processes. The solid line shows the case including wall loss processes of $O(^3P)$, Cl, ClO, and RO_2 (see text).

mental results. This can be easily understood because the chain length of the catalytic cycle should be longer without any wall-loss of radicals. In Fig.4, the solid curve (simulation) and circles (experiment) greatly differ for the latter half of the irradiation time. Probably, unknown secondary products in addition to the above red-mentioned 19 species might have been formed and accumulated, and additional radical reactions may have occur by the photodecomposition of such secondary products.

The solid line in Fig.5 shows the result of a box model simulation of the O3+ CF3Br+h ν system shown in Fig.3. The simulation involved 25 reactions of 11 chemical species. A rate of 2×10^{-3}sec^{-1} was used for the wall-loss processes of O(^{3}P), Br, BrO, and RO2. The agreement between the experiment and simulation is much better than in the case of the Cl system (Fig.4). In the Br system, since the decay of O3 came to completion much faster than in the Cl system, the effect of the formation of unknown secondary products might have been minor.

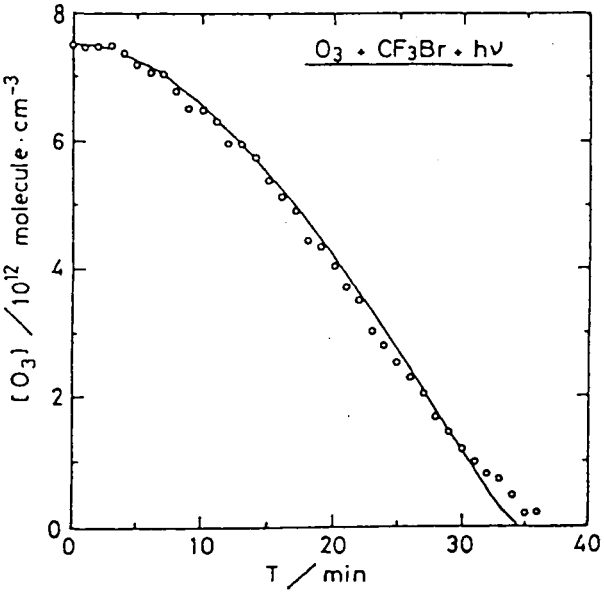

Fig. 5. Result of box model simulation of the O_3+CF_3Br+$h\nu$ system. Circles show experimental results shown in Fig. 5. The solid line shows the result of simulation (see text).

The concentrations of O(^{3}P), Cl, ClO, Br, BrO at the time that 30 and 50% of the initial O3 was decreased ([O3]t = 0.7[O3]0 and [O3]t = 0.5[O3]0) were obtained from the calculation. A remarkable difference between the Cl and Br systems was found at a concentration ratio of [X] to [XO]; i.e., the ratios of [Cl] to [ClO] and [Br] to [BrO] are 1.11×10^{-3} and 3.16×10^{-2} at [O3]t = 0.7[O3]0, and 1.49×10^{-3} and 5.0×10^{-2} at [O3]t = 0.5[O3]0, respectively. In other words, the concentration of Br atoms is remarkably high in the Br system. This fact was caused by the large rate constant of Reaction (11a). From the rate constants of Reaction (6) for Cl and Br, 3.8×10^{-11} and 3×10^{-11} cm^3 molecule^{-1} s^{-1}, respectively, and those for Reactions (10a), (10b), and (11a), and concentrations of [O] and [XO] in Table1, the effective catalytic cycles in both systems could be estimated. In the CFCl3 system, 90% of the catalytic cycle proceeded from Reactions (5) and (6). On the other hand, in the CF3Br system, 90% of the cycle was governed by Reactions (5) and (11a). Therefore, in the present experiment, the CFC system is relatively applicable to the atmosphere.

3 . Temperature Dependence of the Rates of Reaction between Free Radicals with Atomic Oxygen

The rate constant for reactions HS + O(^{3}P) was measured by photoionization mass spectrometry. Each radical was produced by pulsed laser (193 nm) photolysis of H2S and reacted with oxygen atoms produced by microwave discharge of O2 or N2/He. No pressure dependence was observed in the rate constant. Dependence of temperatures on the rate constants was also measured over the temperature range of 186-573K. Results of rate constants are listed in Table 2 together with other radical reactions.

Table 2 Temperature dependence of rate constants for six selected radical-atom reactions.

reaction	rate constant	Temperature range
SH+O→products	$(9.4\pm2.4)\times10^{-11}\exp(111\pm67)/T$	186-343K
NH_2+O→products	$(2.3^{+10.9}_{-1.9})\times10^{-10}\exp(-169\pm501)/T$	242-343K
NH_2+N→products	$(1.5^{+2.3}_{-0.9})\times10^{-10}\exp(-16\pm268)/T$	242-343K
CH_3+N→products	$(1.3\pm0.3)\times10^{-10}\exp(-12\pm62)/T$	188-573K
HNO+O→products	$(4.4\pm2.0)\times10^{-11}\exp(-11\pm127)/T$	242-343K
H_2CN+N→products	$(5.3\pm1.6)\times10^{-11}\exp(-27\pm85)/T$	189-573K

4. Uptake Coefficients of OH to Aqueous Solutions

The heterogeneous reactions are now known to play important role in ozone depletion. The detailed mechanisms and rates, however, are still not fully elucidated, which hinders reliable estimation of the future scenario of the ozone-layer destruction. One of important heterogeneous reaction fields is sulfuric acid aerosol. In liquid heterogeneous reactions, the transport of gas-phase species across the surface (uptake process) is coupled with solution phase reactions. The measurements of uptake coefficient of trace gaseous species from the gas phase is thus very informative. However, because of experimental difficulty, uptake of radical species has been rarely studied so far.

In the present study, the uptake coefficient of OH radicals on aqueous solutions of different pH values has been tried to obtain by a direct method. Namely, in a low pressure vessel, a He gas flow containing OH radicals has been collided with a flow of aqueous solution. The concentration distribution of OH just above the impinging surface, which is determined by the uptake on the aqueous surface, has been measured by means of laser-induced fluorescence method. By analyzing the distribution curve, the uptake coefficient has been obtained. The results are summarized as shown below.

The uptake coefficient of OH on the pH=5.6 aqueous solution is 0.004 under the contact time of 10 -100 ms at 293 K. The coefficient tends to increase both in the acidic and alkaline side. This may be due to the reaction of OH radicals with OH- and HSO4-. However, the quantitative interpretation of the uptake coefficient has been unsuccessful in terms of an aqueous-phase reaction model. Some specific behavior of OH on the surface may be responsible. The fact that the coefficient becomes larger in the acidic side and also at lower temperatures suggests a larger contribution of heterogeneous processes of low-temperature sulfuric acid aerosols. The detailed study of the uptake process is strongly recommended.

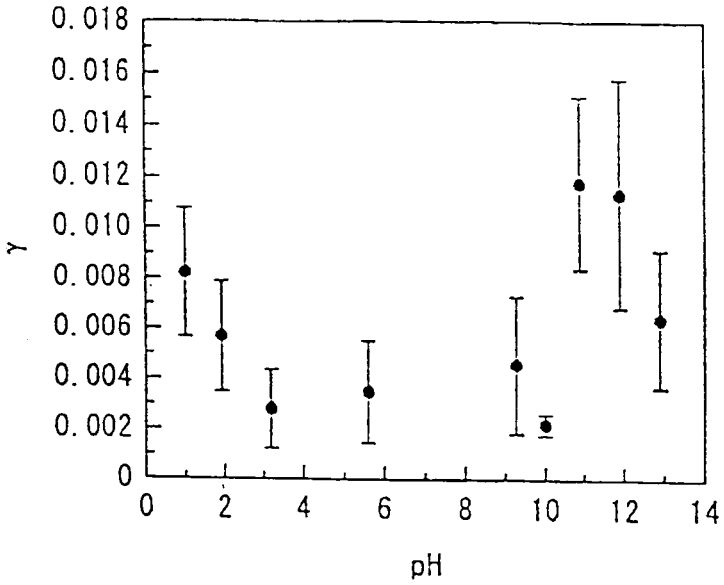

Fig. 6 *pH* dependence of the uptake coefficient of OH. T=293 K, P=70 Torr

4. Simulation of Ozone Destruction due to Heterogeneous Reactions on Sulfuric Acid Aerosols using a 1-D model

We examined the detail of the stratospheric chemical system including heterogeneous reactions by using a 1-D photochemical model on the basis of the aerosol surface area estimated from the measurements. Stratospheric chemical system shifts to a HOx dominant system when the heterogeneous reactions such as N2O5 + H2O and ClONO2 + H2O are included. The source of excess HOx is water in the aerosols. OH enhancement reinforces to convert inactive chlorine to active chlorine. NOx depletion also enhances active chlorine through the reduced reaction rate of ClO + NO2. Ozone loss by enhanced HOx and ClOx was estimated to be about 8% at the peak of the aerosol layer for the Pinatubo aerosol loading. The effects of other heterogeneous reactions of HOx-related species (CH2O, HO2, OH) were also investigated. Simulation shows that in the case of the volcanic eruptions like Mt. Pinatubo ozone reduction due to heterogeneous reactions is about 8% at 20 km.

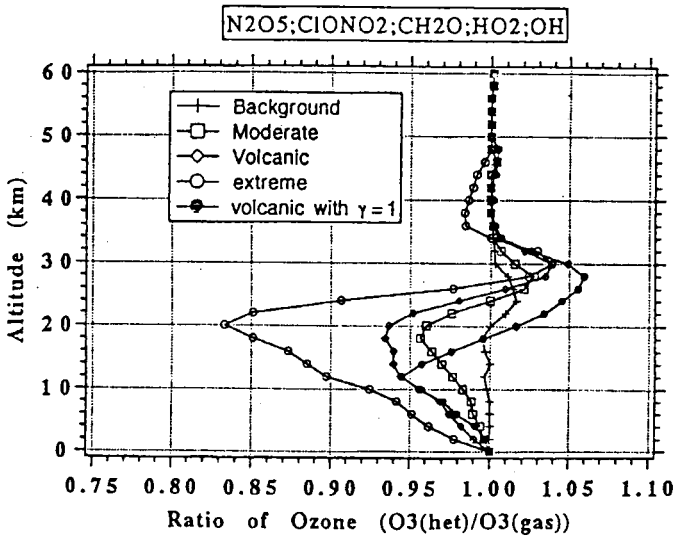

Fig. 7 Ozone reduction due to sulfuric acid aerosols.

5. Simulation of Change of Trace Species in the Ozone Layer due to Injection of Sulfuric Acid using a Full Interactive 1-D model

A one-dimensional chemically radiatively coupled model is developed to study the effects of the stratospheric aerosols on the temperature and concentrations of chemical constituents in the stratosphere. Chemical processes, radiative processes, and the coupled processes between them are explicitly included in the model. A global mean diurnal variation of solar zenith angle is considered on the conditions that the sum of the solar energy received by all portions of the earth surfaces with each solar zenith angle is equal to the solar energy received by the daytime hemisphere of the earth. Simulation shows that in the case of the volcanic eruptions like Mt. Pinatubo ozone reduction due to radiative-chemical coupled processes is 2-3% at 30 km.

6. Publications

Shimono,A. and S.Koda(1995): Laser-spectroscopic measurement of uptake coefficients of gaseouse species on aqueous surfaces. J.Chem.Eng.Japan, 28, 779-785.

Shimono,A. and S.Koda(1996): Laser-spectroscopic measurement of uptake coefficients of SO2 on aqueous surfaces. J.Phys. Chem. in press.

Washida,N., T.Imamura and H.Bandow(1996): Experimental Studies of Ozone Depletion by Chlorofluorocarbons(CFC'S), Bromofluorocarbons(BFC's), Hydrochlorofluorocarbons (HCFC's) and CH3Br Using a 6-m3 Photochemical Chamber. Bull.Chem.Soc.Jpn., 69, 535-541 .